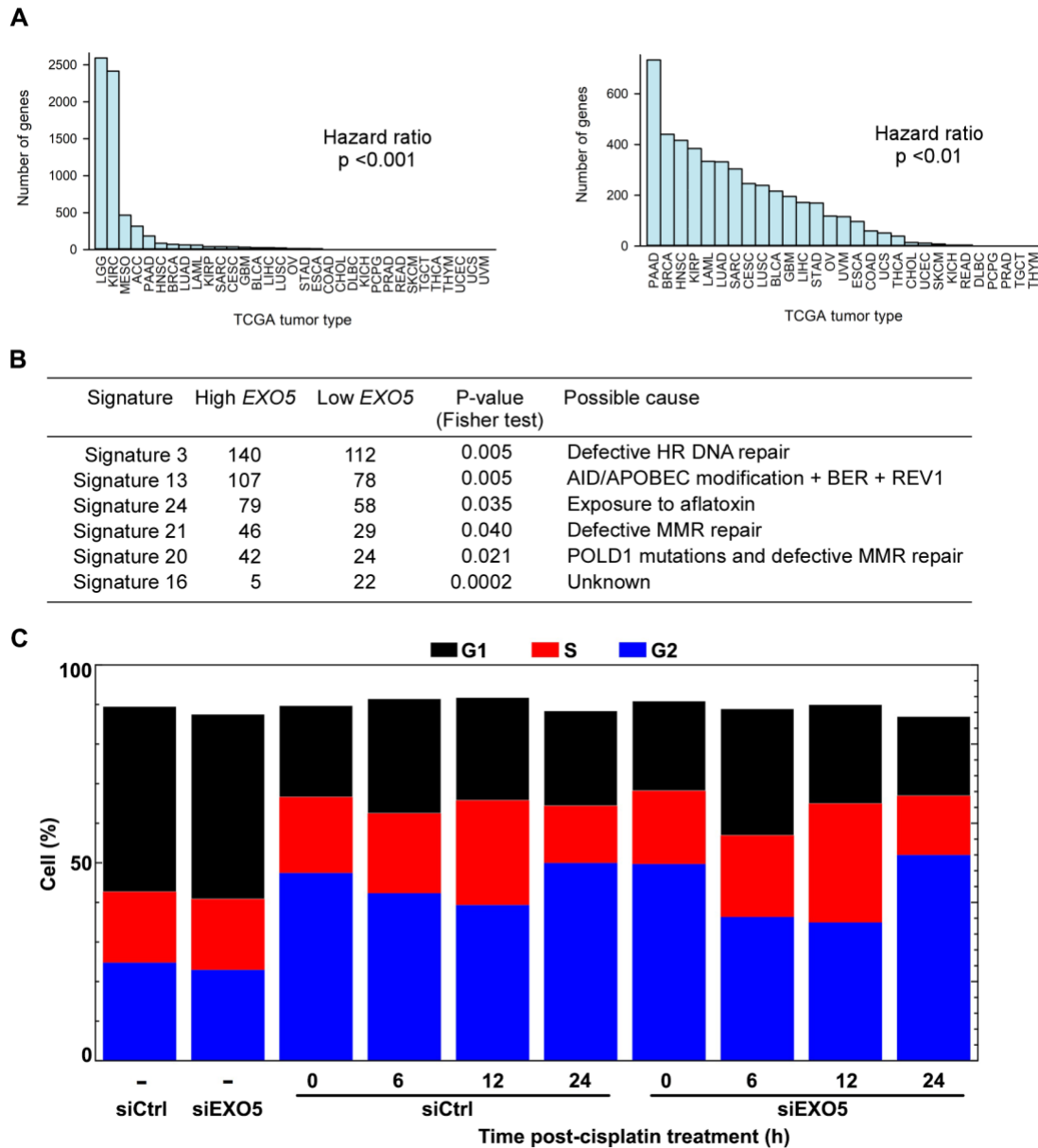
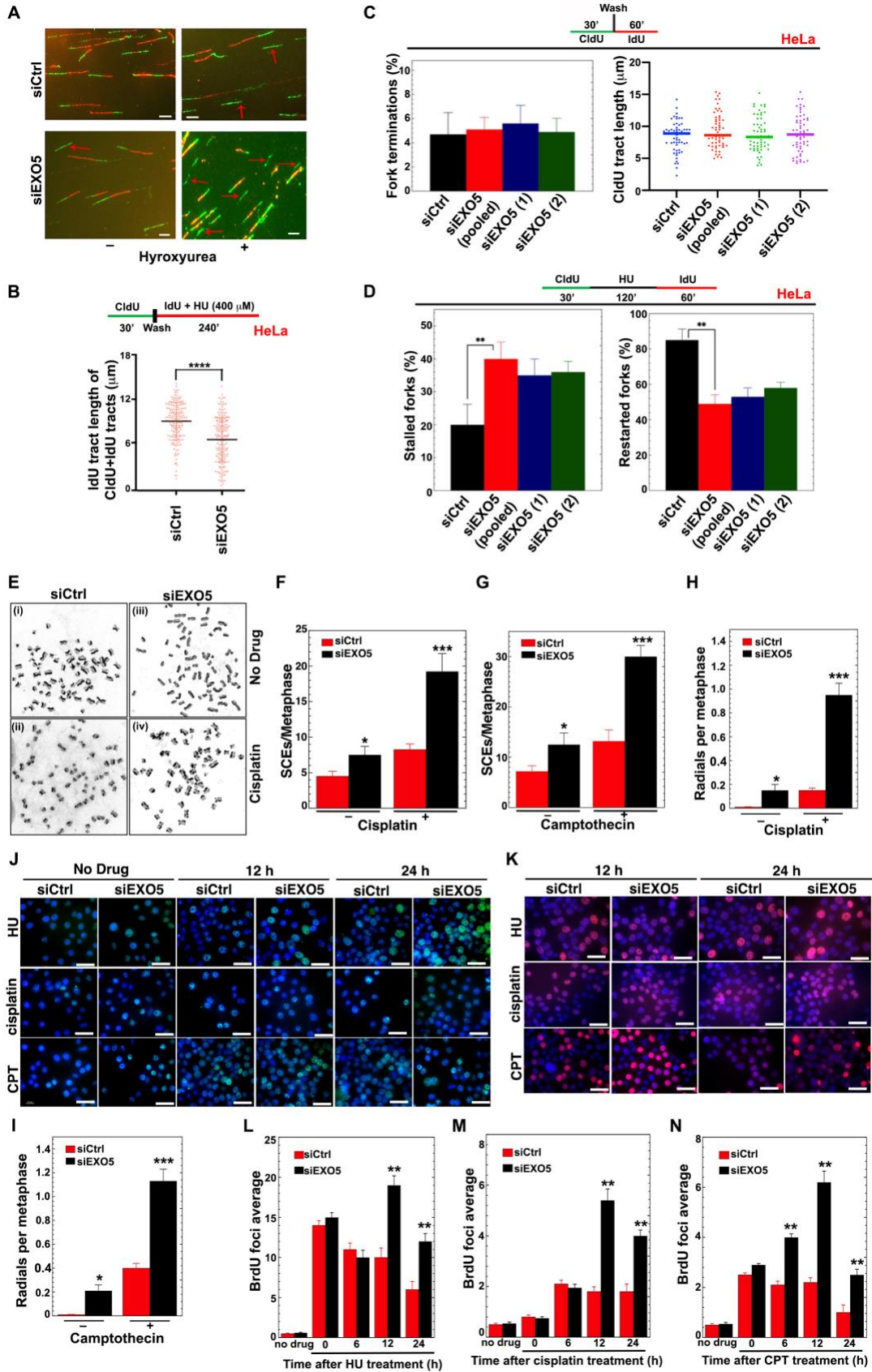


## Supplemental Information



**Figure S1 Related to Figure 1: Genes Expression Associated with Poor Survival, Mutational Signatures, and Cell Cycle of *EXO5***

(A) Bar plots of the number of genes associated with poor survival when expressed at levels above the mean in the tumor samples in TCGA tumors. *Left*, data for all tumors with hazard ratio  $p$ -values  $< 0.001$ ; *right*, data for tumors with hazard ratio  $p$ -values  $< 0.01$  (top 4 tumor types from left panel were omitted). (B) Number of cases among the 200 with the highest and lowest *EXO5* expression in BRCA patients displaying differential signature mutation scores, along with possible mutational signature causes. (C) Cell cycle analysis of propidium iodide stained HeLa cells after removing cisplatin.



**Figure S2 Related to Figure 2: EXO5 Depletion increases Sister Chromatid Exchange, BrdU Foci Formation, and Radials Per Metaphase.**

(A) Representative images of DNA fibers showing CldU green and IdU red labeling. Red arrows point to green-CldU labels referring to (C) and (D), showing the increased frequency of stalled forks in EXO5 KD cells with HU treatment. Scale bar: 5  $\mu$ m. (B) DNA fiber analysis of fork progression in HeLa cells as measured by IdU tract length during hydroxyurea (HU, 400 $\mu$ M) of CldU+IdU fibers; top, experimental scheme. (C) DNA fiber analysis of fork speed (CldU tract length) and termination events without replication stalling [number of CldU tracts without IdU divided by the total number of CldU tracts (CldU plus CldU+IdU tracts)] (n ~50) in HeLa cells; top, experimental scheme. (D) Stalled fork (CldU divided by CldU plus CldU+IdU tracts) and restarted fork (CldU+IdU divided by IdU plus CldU+IdU tracts) percentages in HeLa cells with HU treatment using DNA fiber assay (n~550 fibers per condition); top, experimental scheme. Statistical analysis was performed using the student t test (\*\*  $p<0.01$ ). (E) Representative images of sister chromatid exchange in cells with control siRNA and no drug (i) or cisplatin (ii) treatment, and with EXO5 KD and no drug (iii) or cisplatin (iv) treatment. (F–G) Quantitative analysis of manually counted sister chromatid exchanges (SCE) in cisplatin and CPT treated cells, and data represented as SCE per metaphase. (H–I) Radial chromosomes were manually counted in metaphase spreads of cisplatin or CPT treated cells using light microscope, and data represented as radials per metaphase. (J–K) Representative microscope fields of immunofluorescence staining with (J) anti- $\gamma$ H2AX and (K) anti-RPA1 antibodies. Scale bar: 50  $\mu$ m. (L–N) BrdU foci detection by immunofluorescence staining after terminating the noted drug treatment. The data are averaged from three independent experiments with standard error (\*  $p<0.05$ , \*\*  $p<0.01$ , \*\*\*  $p<0.001$ , \*\*\*\*  $p<0.0001$ ).

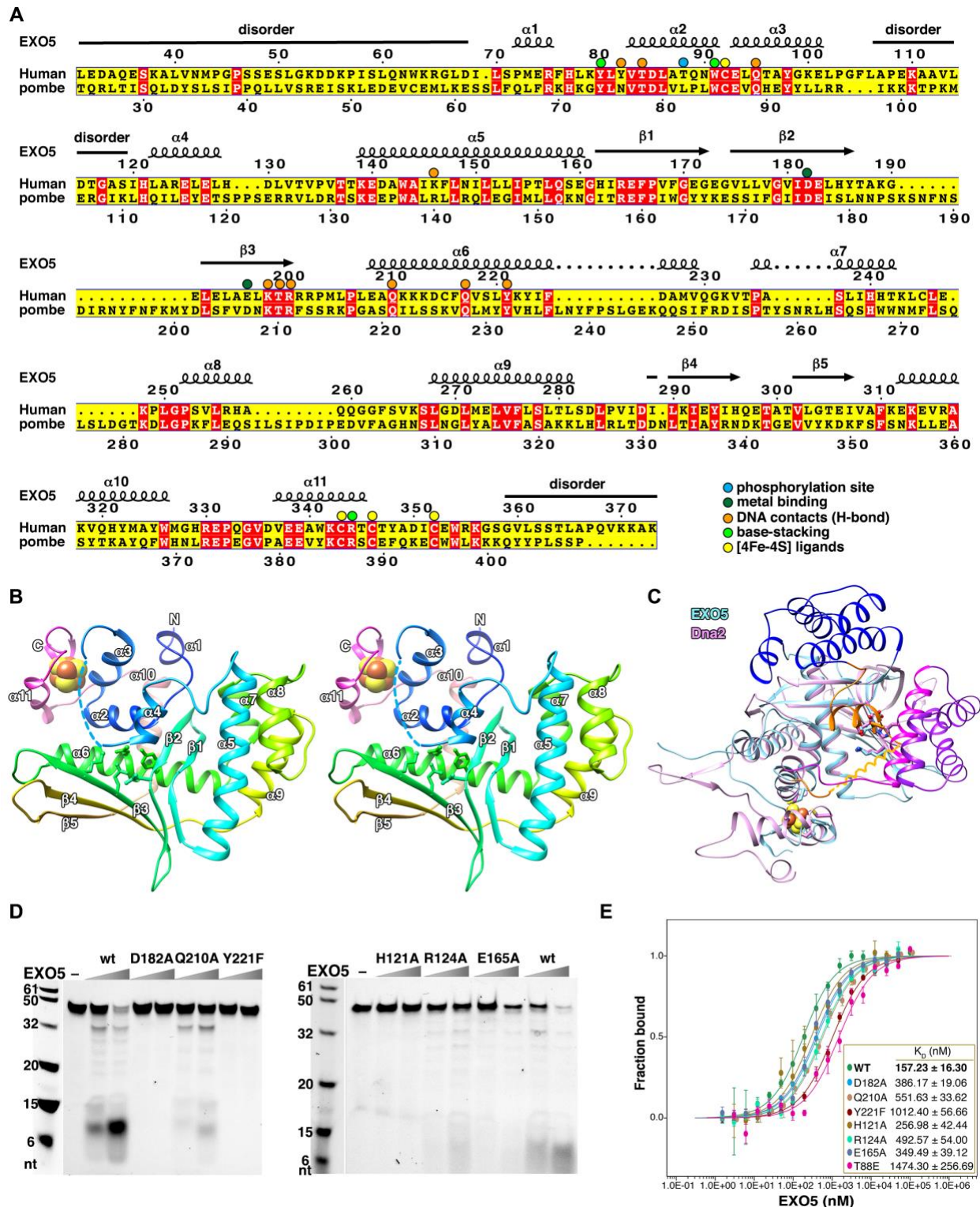


**Figure S3 Related to Figure 4. EXO5 sequence, DNA-free structure, activity, and DNA binding.**

(A) Sequence alignment of EXO5 (DNA-free, 6PMQ) secondary structure and structure elements between human and *S. pombe*. The map was obtained from ESPript 3.0 server

(<http://espript.ibcp.fr/ESPrIPT/cgi-bin/ESPrIPT.cgi>). (B) The overall fold of EXO5 colored in rainbow ribbon from blue (N-ter) to magenta (C-ter) in cross-eye stereoview. (C) Superimposition of EXO5 (6PMQ, light blue) with structurally related DNA2 (5EAN, light pink). The four helix-bundle of EXO5 and corresponding helix-bundle in mouse Dna2 are shown in dark blue and purple, respectively. (D) Impacts of EXO5 mutations on nuclease activity. 3'-Cy5-labeled ssDNA (45 mer) with 5 mM Mg<sup>2+</sup> and different concentrations of EXO5 were incubated at 30 °C for 20 min. (E) DNA binding affinity measurements of EXO5 WT and mutants were done by MST. Data are represented as three independent measurements with standard deviation.



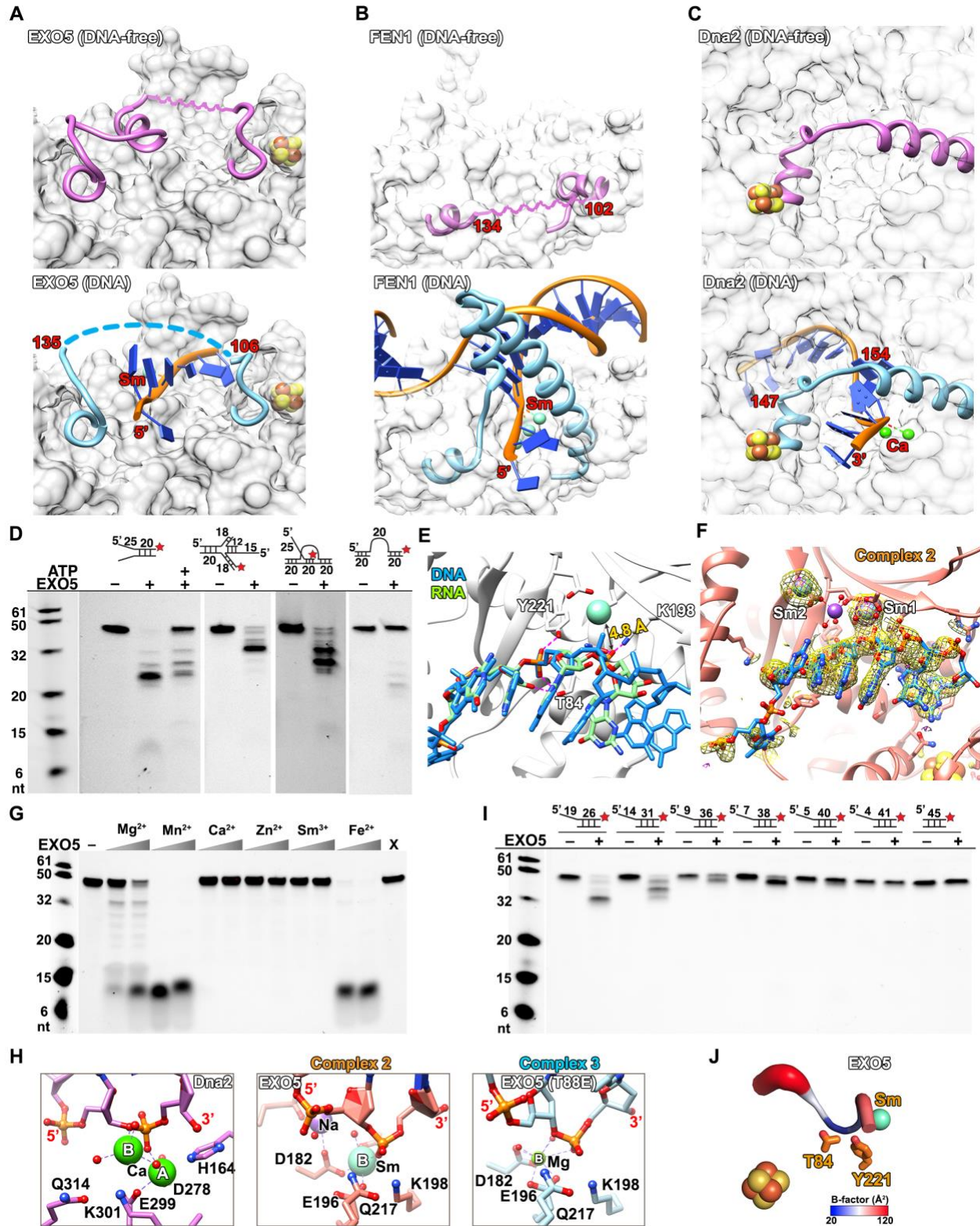


Figure S4 Related to Figure 4. Comparison of EXO5-DNA Complexes with Structure-Related Nucleases.

(A) Comparison of EXO5 DNA-free (top, plum) and complex 2 (bottom, light blue) structures shows the partial-order-to-disorder transition of the crossover-helix. The disordered residues are labeled and presented as spring line and a dash-line. ssDNA is shown in orange ribbon. (B) Comparison of FEN1 DNA-free (top, plum, PDB: 1UL1 chain Y) and DNA-bound complex (bottom, light blue, PDB: 3Q8K) structures shows the disorder-to-order transition of the helical gateway. The disordered residues are labeled. Flap-DNA is shown in orange ribbon. (C) The comparison of Dna2 DNA-free (top, plum, PDB: 5EAW) and DNA-bound complex (bottom, light blue, PDB: 5EAN) structures shows the corresponding crossover-loop. ssDNA is shown in orange ribbon. (D) Processing of different DNA substrates by EXO5 (150 nM). The star represents 3'-Cy5-label. The reaction mixture was incubated at 30 °C for 20 min. The figure is composited from two different gel images. (E) Overlay of RNA (green sticks, modeled) and DNA (blue sticks) in EXO5 complex 2 structure. RNA were fitted and refined based on DNA density map, resulting in RNA scissile phosphate 4.8 Å away from metal ion. (F) The  $2F_o - F_c$  simulated-annealing omit map of EXO5-DNA complex 2 structure at  $1\sigma$ -contour shown in gold mesh. The anomalous density map shown in purple mesh is at  $3\sigma$ -contour. DNA: blue sticks; Sm: teal sphere; Na: purple sphere; water: red sphere. The electron density of Na and its bound water is not shown. (G) Metal-dependent nuclease activity of EXO5. The resection of 3'-Cy5-labeled ssDNA (45 mer) by different EXO5 concentrations (0, 75, 150 nM) was initiated by adding the metal ion (5 mM) and incubated at 30 °C for 20 min. (H) The metal binding site of mouse-Dna2 (left panel, PDB: 5EAN), EXO5 Complex 2 (middle panel), and EXO5 Complex 3 (T88E, right panel) structures. (I) Footprint nuclease assay to measure the minimum substrate length for EXO5 end-resection. The reaction mixture with or without EXO5 (150 nM) was incubated at 30 °C for 20 min. (J) DNA anchoring by residues Y221 and T84 in Complex 2 structure. DNA is shown in putty colored by B-factor (blue, most rigid; red, most flexible).





**Figure S5 Related to Figure 5. EXO5 and BLM Epistatic Genetic Relationship in Fission Yeast that Is Conserved in Human to Promote DNA Resection.**

(A–E) Western blots showing siRNA KD efficiency in HeLa cells for mentioned proteins. Anti-EXO5 antibody used for detecting endogenous expression. (F–G) Clonogenic cell survival assay in HEK293 cells with (F) CPT and (G) HU treatment with KD of EXO5, BLM or EXO5/BLM. Western blot with mentioned antibodies show KD efficiency in HEK293 cells. (H) CldU-labeled fiber lengths were measured to detect replication fork degradation for EXO5 and/or BLM depleted cells with or without HU treatment in HeLa cells (experimental scheme above plot). The average of three independent experiments is shown (\*\*\*\*  $p < 0.0001$ ). (I–K) Clonogenic cell survival assay for mentioned protein KD in HEK293 cells with HU treatment. Western blot show KD efficiency of mentioned proteins in HEK293 cells (\*  $p < 0.05$ , \*\*  $p < 0.01$ ). (L) Exo5 genetic interaction analyses in fission yeast with genetic KOs. Exo5 functions primarily in a pathway requiring Pso2 (SNM1) and Rad13 (XPG), but independent of Fan1 (FAN1). (M) The *exo5* $\Delta$  and *rqh1* $\Delta$  (BLM/WRN) mutants are sensitive to cisplatin, and the combination of the mutations has no additive effect. 5-fold serial dilutions of log-phase cells on YES media with the indicated genotype were exposed to indicated dose of cisplatin. Plates were photographed after 3 days at 30 °C. (N) EXO5 end-resection on fork substrate with BLM<sub>cat</sub> and RPA domains. The reaction mixture were incubated at 30 °C for 30 min. The star represents the Cy5-label at 3'-end. (O) Quantitative analysis of DNA resection by EXO5 with BLM<sub>cat</sub> and RPA70NAB in Figure 5M. (P) EXO5 end-resection on D-loop substrate. Same condition as (N).

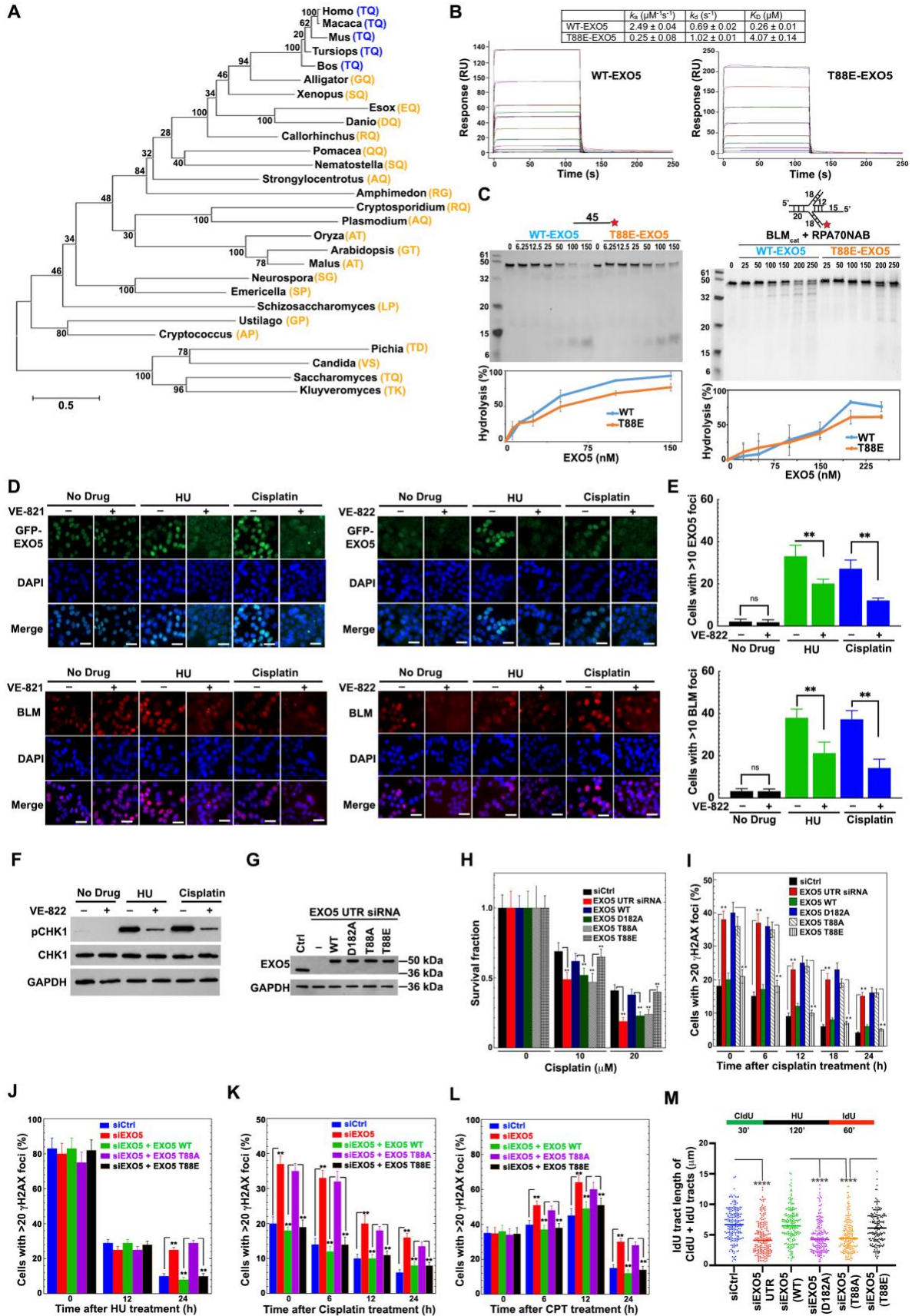


**Figure S6 Related to Figure 6. EXO5 Phosphorylation Is Required for Efficient ssDNA End-Resection and Recovery from DNA Damage.**

(A) Evolutionary tree of *EXO5*. Branch lengths is proportional to the number of substitutions per site. Numbers indicate the percentage of trees in which the associated taxa clustered together from the Bootstrap method. Blue, conserved TQ dipeptide in mammals. (B) DNA binding kinetics of WT and T88E-*EXO5* measured by surface plasma resonance. The plots show the sensorgrams of titrated *EXO5* concentration corresponding to response unit (RU) and the fitted kinetic results (two independent experiments). (C) Left panel: *EXO5* nuclease activity comparison between WT and T88E mutant at different concentrations shown in (top) TBE-urea gel and (bottom) plotted in hydrolysis (%) in three independent experiments at 30° C for 20 min. Right panel: *EXO5* variant nuclease activity in the presence of BLM<sub>cat</sub> and RPA70NAB (in 1:1:1 molar ratio) at different concentrations shown in TBE-urea gel (top) and hydrolysis (%) (bottom) in two independent experiments at 30° C for 20 min. (D) Representative images of GFP-*EXO5* foci (top) and BLM foci (bottom) 12h after removing HU (2 mM for 24h) or cisplatin (20 μM for 1h) in presence or absence of VE-821 or VE822 in HeLa cells. DAPI stain for detecting nuclei. Scale bar: 50 μm. (E) Quantitative analysis of GFP-*EXO5* foci and BLM foci induced by drugs as mentioned in (D) in presence or absence of VE-822. (F) Western blot showing phospho-CHK1 level under mentioned drug conditions and presence or absence of VE-822 ATR inhibitor. Drug concentrations and time of analysis were the same as described in (D). (G) Western blot showing KD of endogenous *EXO5* (~41 kDa band) using UTR specific siRNA and transient expression of WT and mutant HA-Flag-*EXO5* (~49 kDa band). Anti-*EXO5* antibody detects *EXO5* expression. (H) Clonogenic survival assay for HEK293 cells with knock-down of endogenous *EXO5* and expression of mutants and WT *EXO5* (\*\*  $p < 0.01$ ). (I) Analysis of γ-H2AX foci formation in presence of WT and mutant *EXO5* after terminating noted drug treatment in HEK293 and (J–L) in HeLa cells. (M) DNA fiber assay determining fork recovery in HEK293 cells with KD of endogenous *EXO5* and expression of WT and mutant *EXO5*. Data is the average of three-independent experiments (\*\*  $p < 0.01$ , \*\*\*\*  $p < 0.0001$ ).

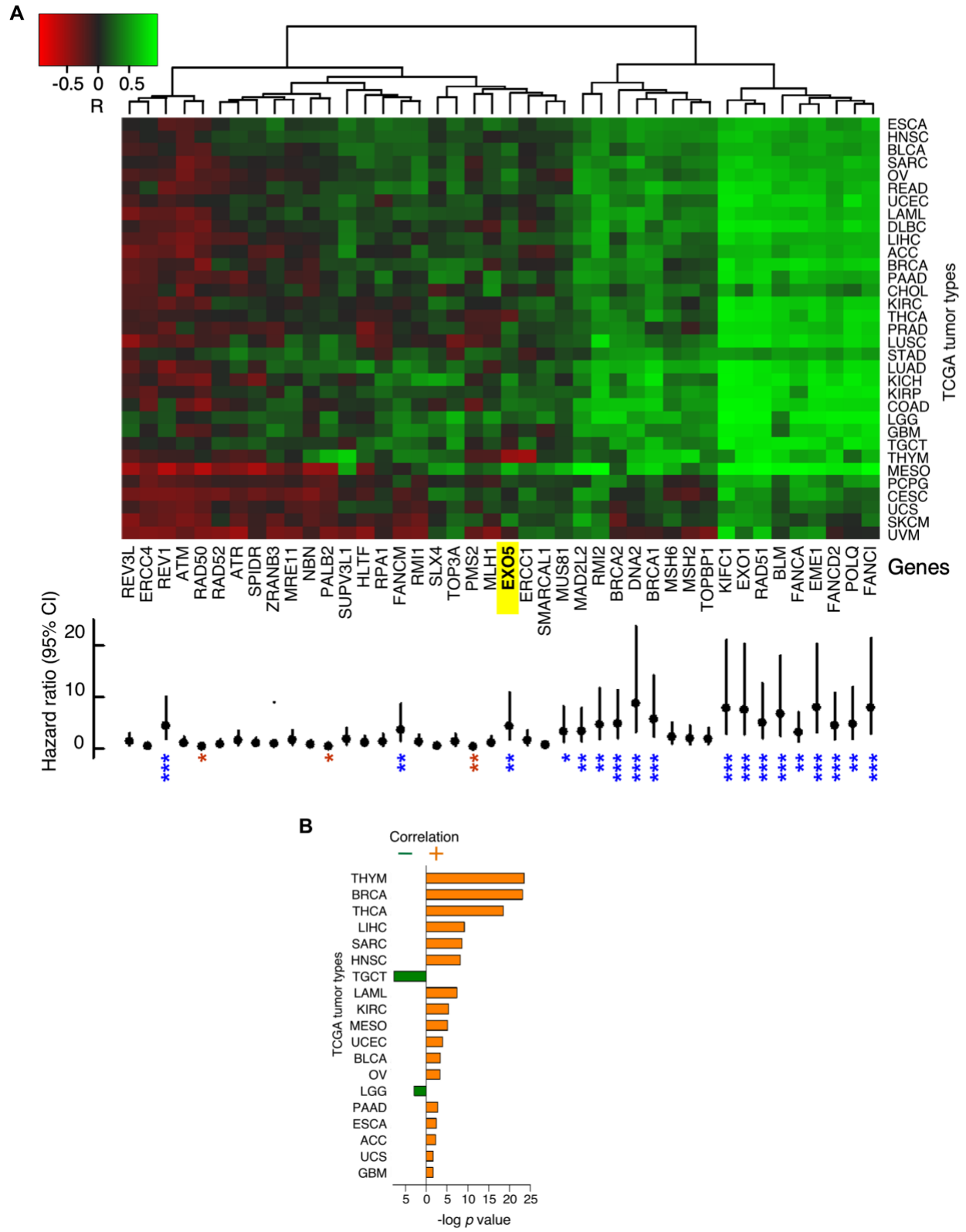


Figure S7 Related to Figure 7. Poor Cancer Prognosis Correlates with *BLM* and *FA* Overexpression



(A) Top, Euclidean hierarchical clustering and heatmap of regression coefficients from correlations in gene expression between *MYBL2* (transcription factor and marker for cell proliferation) and DNA repair genes in 33 TCGA tumor types. *Green*, positive correlations, *red*, negative correlations. *KIFC1*, positive control for gene transactivated by MYBL2. Bottom, hazard ratios in ACC patients for genes in the top panel. *P*-values: \*\*\* <0.001; \*\* <0.01; \* <0.05. Blue, worse survival for high expression; red, worse survival for low expression. (B) Significant *p*-values for correlations in gene expression between *EXO5* and *BLM* in TCGA tumors from Welch's t-tests.

**Table S1 Related to Figure 3. Top 20 proteins detected by LC-MS/MS analysis of Flag-EXO5 immunoprecipitated proteins.**

Gene symbol	Peptides
<b>EXO5</b>	52
<b>RPA1</b>	12
CANX	10
SSBP1	10
ENAH	6
BAG2	5
<b>BLM</b>	5
MCM3	5
DNAJC7	5
SFXN3	5
ACTR3	4
TOP3A	4
ECD	4
GPS1	4
PNPT1	4
XPO1	3
ISG15	3
AGK	3
SFXN2	3
HAUS1	3

**Table S2 Related to KEY RESOURCES TABLE. Oligonucleotides**

REAGENT or RESOURCE	SOURCE	IDENTIFIER
Oligonucleotides		
EXO5 siRNA Pooled	Dharmacon GE (Davis et al., 2013)	Cat#M-014212-00-0005
EXO5 siRNA (1): ACUCAGAACUGGUGUGAACUU+GUUCACACCAGUU CUGAGUUU	Sparks et al., 2012	ORF176-1
EXO5 siRNA (2): CUGUGAAGUCUUUGGGUGAUU+UCACCCAAAGAC UUCACAGUU	Sparks et al., 2012	ORF176-2
EXO5 UTR siRNA	Dharmacon GE	Cat#J-014212-20-0005
BLM siRNA	Dharmacon GE (Garzon et al., 2019)	Cat#L007287-00-0005 (Garzon et al., 2019)
EXO1 siRNA	Dharmacon GE (Garzon et al., 2019)	Cat#L-013120-00-0005
DNA2 siRNA	Dharmacon GE (Garzon et al., 2019)	Cat#L-026431-01-0005
Mre11 siRNA	Dharmacon GE (Lemacon et al., 2017)	Cat#L-009271-00-0005
Mus81 siRNA	Dharmacon GE (Cristini et al., 2019)	Cat#L-016143-01-0005
FANCA siRNA	Dharmacon GE (Benitez et al., 2018)	Cat#L-019283-00-0005
FANCD2 siRNA	Dharmacon GE (McLaughlin et al., 2020)	Cat#L-016376-00-0005
SMARCAL1 siRNA	Dharmacon GE (Nieminuszczy et al., 2019)	L-013058-00-0005
Control siRNA	Dharmacon	D-001810-01
12-mer dT12: 5' TTTTTTTTTTTTT/3ThioMC3-D/ 3'	Integrated DNA Technologies	N/A
12-mer: ATT GCT GAA GGG	Integrated DNA Technologies	N/A
45-mer 3'-Cy5 label: CCACCTGTGATTACTTTGAGGCAGAGTCCATGTCAA GCAGTCCTA/3Cy5/	Integrated DNA Technologies	N/A
RF1: ACGCTGCCGAATTCTACCAGTGCCTTGCTAGGACAT CT	Integrated DNA Technologies	N/A
RF2: TAGGACTGCTTGACATGGCTGGTAGAATTCGGCAG CGT	Integrated DNA Technologies	N/A
RF3: AGATGTCCTAGCAAGGCAACTCTGCCTCAA	Integrated DNA Technologies	N/A

D-loop-1: GGGTGAACCTGCAGGTGGGCTAGGACTGCTTGACA TGGACTTGGTAGAATTCGGCAGCGT	Integrated DNA Technologies	N/A
D-loop-2: ACGCTGCCGAATTCTACCATTCTTTCTCTTTTTTCT TCTGCCACCTGCAGGTTCACCC	Integrated DNA Technologies	N/A
Fork: TAG GAC TGC TTG ACA ATT TTT TTT TTT TTT TTT TTT TTT TTT TTT	Integrated DNA Technologies	N/A
Gap-1: TAG GAC TGC TTG ACA	Integrated DNA Technologies	N/A
Gap-2: AGT AAT CAC AGG TGG	Integrated DNA Technologies	N/A
Footprint-26: TAG GAC TGC TTG ACA TGG ACT CTG CC	Integrated DNA Technologies	N/A
Footprint-31: TAG GAC TGC TTG ACA TGG ACT CTG CCT CAA A	Integrated DNA Technologies	N/A
Footprint-36: TAG GAC TGC TTG ACA TGG ACT CTG CCT CAA AGT AAT	Integrated DNA Technologies	N/A
Footprint-38: TAG GAC TGC TTG ACA TGG ACT CTG CCT CAA AGT AAT CA	Integrated DNA Technologies	N/A
Footprint-40: TAG GAC TGC TTG ACA TGG ACT CTG CCT CAA AGT AAT CA	Integrated DNA Technologies	N/A
Footprint-41: TAG GAC TGC TTG ACA TGG ACT CTG CCT CAA AGT AAT CAC AG	Integrated DNA Technologies	N/A
Footprint-45: TAG GAC TGC TTG ACA TGG ACT CTG CCT CAA AGT AAT CAC AGG TGG	Integrated DNA Technologies	N/A